Article ID: 1007-4627(2014) 03-0315-011

Ratio of Shear Viscosity to Entropy Density of Nuclear Participant in the Intermediate Energy Heavy Ion Collisions

MA Yugang, ZHOU Chenglong, FANG Deqing

(*Shanghai Institute of Applied Physics, Chinese Academy of Sciences, Shanghai 201800, China*)

Abstract: The ratio of shear viscosity (η) to entropy density (s) of nuclear fireball created in the central region of intermediate-energy heavy-ion collisions has been investigated within two transport models, namely the Boltzmann-Uehling-Uhlenbeck (BUU) model and the isospin-dependent quantum molecular dynamics (IQMD) model. Different methods are used to calculate η and s. With the collision energy increasing, the η/s displays a saturation value or a local minimum value at a certain beam energy. We argue that the saturation or minimum point corresponds to an occurrence of nuclear liquid gas phase transition.

Key words: shear viscosity; entropy density; heavy ion collision; transport model

CLC number: O572.21 **Document code:** A **DOI:** 10.11804/NuclPhysRev.31.03.315

1 Introduction

In the past decades, extensive experimental and theoretical efforts have been devoted to search for the nuclear liquid-gas phase transition (LGPT) in intermediate energy heavy-ion collisions (HIC)[1–12]. Many probes have been suggested for the onset of nuclear LGPT, for instance, the fragment size distribution[13] and its rank distribution[12], the largest fluctuation of the heaviest fragment[14], caloric curve[4, 6], bimodality[15] *etc.* In addition, it has been observed that the ratio of shear viscosity to entropy density (η/s) reaches its local minimum at the transition temperature for a wide class of systems. For instance, empirical observation of the temperature or incident energy dependence of the shear viscosity to entropy density ratio for H_2O, He and Ne_2 exhibits a minimum in the vicinity of the critical point for phase transition[16]. And more recently, a lower bound of $\eta/s > 1/4\pi$ obtained by Kovtun-Son-Starinets (KSS) for infinitely coupled super-symmetric Yang-Mills gauge theory based on the AdS/CFT duality conjecture, is speculated to be valid universally[17−18].

In ultra-relativistic HIC[19–23], people have used the ratio of shear viscosity to entropy density to study the quark-gluon plasma phase and the extracted value of η/s seems very close to the KSS bound ($1/4\pi$). In intermediate energy heavy-ion collision, several pieces of work have been done on different models[24–31]. In our previous papers[27−28], simulations on central Au+Au collisions have been performed for investigating the shear viscosity over entropy density ratio by using two microscopic transport models known as the isospin-dependent quantum molecular dynamics (IQMD) model[32–37] and the Boltzmann-Uehling-Uhlenbeck (BUU)[38–41] model. In this paper we would like to make a brief summary on the above work. The focus is on the relationship between η/s and the nuclear liquid gas phase transition. Different kinds of

Received date: 25 Sep. 2013; **Revised date:** 18 Oct. 2013

Foundation item: National Natural Science Foundation of China(11035009, 11220101005), National Basic Research Program of China (973 Program)(2013CB834405)

Biography: MA Yugang(1968–), male, Shanghai, China, Professor, working on the field of nuclear physics;
E-mail: ygma@sinap.ac.cn.

method are used to extract the related thermal and transport properties, including the generalized hot Thomas Fermi formalism (GHTFF)[42–44], the momentum fluctuation[45], Green-Kubo formula, transport formula[46] and so on. At last the multiplicity of intermediate mass fragment (IMFs) is also investigated as a signal of liquid gas phase phase transition[47–50] to verify the calculation results.

The paper is organized as follows. Section 2 provides a brief introduction for the IQMD and BUU models. Section 3 introduces the different calculation methods used to extract the thermal and transport properties. In Section 4 we present the calculation results and discussions.

2 IQMD and BUU models

2.1 BUU

BUU model is a one-body microscopic transport model based upon the Boltzmann equation[38−39]. The BUU equation reads [40]

$$\frac{\partial f}{\partial t}+v\cdot\nabla_r f-\nabla_r U\cdot\nabla_p f=\frac{4}{(2\pi)^3}\int \mathrm{d}^3p_2\mathrm{d}^3p_3\mathrm{d}\Omega \frac{\mathrm{d}\sigma_{\mathrm{NN}}}{\mathrm{d}\Omega}V_{12}\times\Big[f_3f_4(1-f)(1-f_2)-ff_2(1-f_3)\times(1-f_4)\Big]\delta^3(p+p_2-p_3-p_4)\ . \quad (1)$$

It is solved with the method of Bertsch and Das Gupta[41]. In Eq. (1), $\mathrm{d}\sigma_{\mathrm{NN}}/\mathrm{d}\Omega$ and V_{12} are in-medium nucleon-nucleon cross section and relative velocity for the colliding nucleons, respectively, and U is the mean field potential including the isospin-dependent term:

$$U(\rho,\tau_z)=a(\frac{\rho}{\rho_0})+b(\frac{\rho}{\rho_0})^\sigma+C_{\mathrm{sym}}\frac{(\rho_{\mathrm{n}}-\rho_{\mathrm{p}})}{\rho_0}\tau_z\ , \quad (2)$$

where ρ_0 is the normal nuclear matter density; ρ, ρ_{n}, and ρ_{p} are the nucleon, neutron and proton densities, respectively; τ_z equals 1 or -1 for neutrons and protons, respectively; The coefficients a, b and σ are parameters for nuclear equation of state. Two sets of mean field parameters are used in this work, namely the soft EOS with the compressibility K of 200 MeV ($a=-356$ MeV, $b=303$ MeV, $\sigma=7/6$), and the hard EOS with K of 380 MeV ($a=-124$ MeV, $b=70.5$ MeV, $\sigma=2$). C_{sym} is the symmetry energy strength due to the density difference of neutrons and protons in nuclear medium, here $C_{\mathrm{sym}}=32$ MeV is used.

2.2 IQMD

On the other hand, the QMD approach is a many-body theory that describes heavy-ion collisions from intermediate to relativistic energy[32]. The IQMD model[33−34] is based on the QMD model, including the isospin degrees and Pauli blocking *etc.* Each nucleon in the colliding system is described as a Gaussian wave packet

$$\phi_i(\boldsymbol{r},t)=\frac{1}{(2\pi L)^{3/4}}\times\exp\left[-\frac{(\boldsymbol{r}-\boldsymbol{r}_i(t))^2}{4L}\right]\exp\left[-\frac{\mathrm{i}\boldsymbol{r}\cdot\boldsymbol{p}_i(t)}{\hbar}\right]\ . \quad (3)$$

Here $\boldsymbol{r}_i(t)$ and $\boldsymbol{p}_i(t)$ are the mean position and mean momentum, respectively, and the Gaussian width has the fixed value $L=2.16$ fm^2 for Au+Au system. The centers of these Gaussian wave packets propagate in coordinate ($\boldsymbol{R}$) and momentum ($\boldsymbol{P}$) space according to the classical equations of motion:

$$\boldsymbol{p}_i=-\frac{\partial\langle\boldsymbol{H}\rangle}{\partial\boldsymbol{r}_i};\quad \boldsymbol{r}_i=\frac{\partial\langle\boldsymbol{H}\rangle}{\partial\boldsymbol{p}_i}\ , \quad (4)$$

where $\langle\boldsymbol{H}\rangle$ is the Hamiltonian of the system.

The Wigner distribution function for a single nucleon density in phase space is given by

$$f_i(\boldsymbol{r},\boldsymbol{p},t)=\frac{1}{\pi^3\hbar^3}\mathrm{e}^{-(\boldsymbol{r}-\boldsymbol{r}_i(t))^2\frac{1}{2L}}\mathrm{e}^{-(\boldsymbol{p}-\boldsymbol{p}_i(t))^2\frac{2L}{\hbar^2}}. \quad (5)$$

The mean field in IQMD model is:

$$U(\rho)=U_{\mathrm{Sky}}+U_{\mathrm{Coul}}+U_{\mathrm{Yuk}}+U_{\mathrm{sym}}, \quad (6)$$

where U_{Sky}, U_{Coul}, U_{Yuk}, and U_{sym} represents the Skyrme potential, the Coulomb potential, the Yukawa potential and the symmetry potential interaction, respectively[32]. The Skyrme potential is:

$$U_{\mathrm{Sky}}=\alpha(\rho/\rho_0)+\beta(\rho/\rho_0)^\gamma, \quad (7)$$

where $\rho_0=0.16$ fm^{-3} and ρ is the nuclear density. In the present work, the parameter set with $\alpha=-356$ MeV, $\beta=303$ MeV, and $\gamma=7/6$, is used, which corresponds to a soft equation of state. U^{Yuk} is a long-range interaction (surface) potential, and takes the following form

$$U^{\rm Yuk}=\frac{V_y}{2}\sum_{i\neq j}\frac{\exp(Lm^2)}{r_{ij}}\cdot \left[\exp(mr_{ij})erfc\left(\sqrt{L}m-\frac{r_{ij}}{\sqrt{4L}}\right)-\exp(mr_{ij})erfc\left(\sqrt{L}m+\frac{r_{ij}}{\sqrt{4L}}\right)\right] \quad (8)$$

with $V_y=0.0074$ GeV and $m=1.25$ fm^{-1}. r_{ij} is the relative distance between two nucleons. The symmetry potential is $U_{\rm sym}=32(\rho_{\rm n}-\rho_{\rm p}/\rho_0)\tau_z$ MeV, where $\rho_{\rm n}$, $\rho_{\rm p}$, and ρ_0 are the neutron, proton and nucleon densities, respectively; τ_z equals 1 or -1 for neutrons and protons, respectively.

From Eq. (5) one obtains the matter density of coordinate space by the sum over all the nucleons, *i.e.*

$$\rho(\boldsymbol{r},t)=\sum_{i=1}^{A_{\rm T}+A_{\rm P}}\rho_i(\boldsymbol{r},t)=\sum_{i=1}^{A_{\rm T}+A_{\rm P}}\frac{1}{(2\pi L)^{3/2}}{\rm e}^{-\frac{(\boldsymbol{r}-\boldsymbol{r}_i(t))^2}{2L}} . \quad (9)$$

The kinetic energy density in coordinate space could also be calculated from Eq. (9)

$$\rho_K(\boldsymbol{r},t)=\sum_{i=1}^{A_{\rm T}+A_{\rm P}}\frac{\boldsymbol{P}_i(t)^2}{2m}\rho_i(\boldsymbol{r},t) . \quad (10)$$

The time evolution of the mean nuclear density and kinetic energy density in a given central volume (with $R=3.5$ fm) is shown in Fig. 1. Both the matter density and kinetic energy density are reaching their maxima around 20 fm/c. And the hot and dense nuclear matter survives for a longer time when the beam energy is lower. This can be easily understood as the nuclear matter experiences compressed and expanded processes more quickly at higher beam energy.

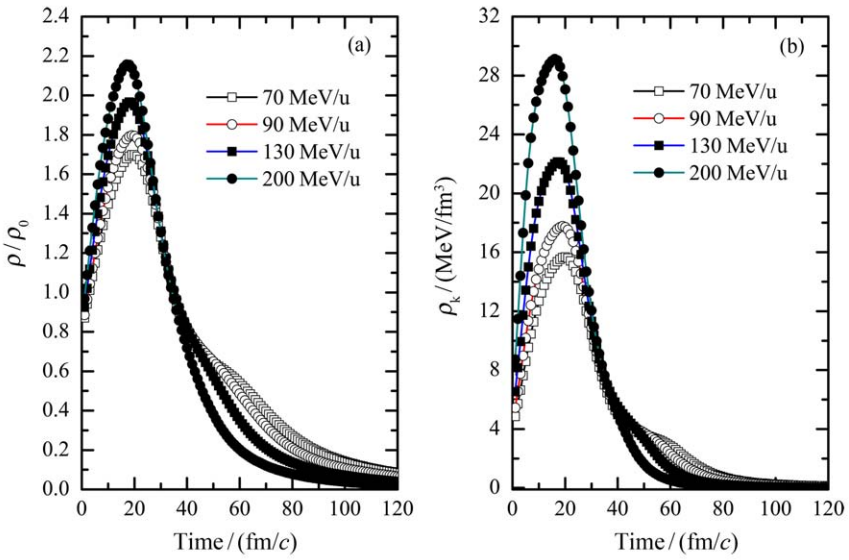

Fig. 1　(color online) The time evolution of mean nuclear matter density (a) and kinetic energy density (b) in a central region defined as a sphere with radius $R=3.5$ fm for the head-on Au+Au collisions in the QMD model. Different symbols represent different beam energies which are illustrated in the inset.

3　Calculation formula

3.1　The Generalized Hot Thomas-Fermi Formalism

Thermodynamical properties of hot nuclear matter formed in heavy ion collisions, *e.g.* temperature and entropy density, can be extracted by using the approach developed by Faessler and collaborators[42−44, 51−52]. In this approach one starts from a microscopic picture of two interpenetrating pieces of nuclear matter and deduces thermal quantities from the matter density and kinetic energy density obtained during the collisions. In this paper, the extraction of thermal properties of the hot nuclear matter is done in two steps. First, based on the IQMD simulation, one can calculate the nuclear matter density and kinetic energy density at each point in coordinate space at every time step. Second, by

employing the hot Thomas-Fermi formalism, one can obtain the corresponding thermal properties for every set of nuclear matter density and nuclear kinetic energy density[42−43]. In GHTFF, the momentum distribution in cylindrical coordinates k_r, k_z can be written as

$$n(K)=\begin{cases} n1(K)=\left\{1+\exp\left[\dfrac{\hbar^2(k_r^2+k_z^2)}{2mT-\mu_1'}\right]\right\}^{-1}, & k_z<k_0 \\ n2(K)=\left\{1+\exp\left[\dfrac{\hbar^2\left[k_r^2+(k_z-k_{\rm R})^2\right]}{2mT-\mu_2'}\right]\right\}^{-1}, & k_z>k_0 \end{cases}$$

with $\mu_i'=\mu_i/T$ is the reduced chemical potential, $k_0=[k_{\rm R}^2-2mT(\mu_1'-\mu_2')]/2k_{\rm R}$, $k_{\rm R}$ is the relative momentum between the projectile (index 1) and target (index 2). The local nuclear matter density ρ_i is expressed as

$$\rho_i=\frac{1}{2}\rho_0(\mu_i')+\frac{1}{2\pi^2}\left(\frac{2mT}{\hbar^2}\right)^{3/2}\left[f(\mu_i',K_{0i})+J_{1/2}(\mu_i',K_{0i}^2)\right] , \tag{11}$$

where $K_{01}=\hbar K_0/\sqrt{2mT}, K_{02}=K_{\rm R}-K_{01}$ with $K_r=\hbar k_{\rm R}/\sqrt{2mT}$, and $J_n(\mu')=J_n(\mu',\infty)$ is the Fermi integrals, *i.e.*

$$J_n(\mu',z)=\int_0^z\frac{x^n{\rm d}x}{1+\exp(x-\mu')},\quad f(\mu_i',K_{0i})=K_{0i}\ln\left[1+\exp(\mu_i'-K_{0i}^2)\right] .$$

The local kinetic energy density $\epsilon=\hbar^2\tau_i/(2m)$, where τ_i reads

$$\tau_i=\frac{1}{2}\tau_0\left(\mu_i'\right)+\frac{1}{2\pi^2}(\frac{2mT}{\hbar^2})^{5/2}\left[\frac{1}{3}K_{0i}^2f(\mu_i',K_{0i})+\frac{1}{3}J_{1/2}(\mu_i',K_{0i}^2)+\int_0^{K_{0i}}J_1(\mu_i'-x^2){\rm d}x\right]+\Delta\tau_i(\mu_i') . \tag{12}$$

And the entropy density s_i is written as

$$\begin{aligned} s_i=&\frac{1}{2}s_0(\mu_i')+\frac{1}{2\pi^2}\left(\frac{2mT}{\hbar^2}\right)^{3/2}\left[\left(\frac{1}{3}K_{0i}^2-\mu_i'\right)f\left(\mu_i',K_{0i}\right)+\right. \\ &\left.\frac{1}{3}J_{1/2}(\mu_i',K_{0i}^2)-\mu_i'J_{1/2}(\mu_i',K_{0i}^2)+2\int_0^{K_{0i}}J_1(\mu_i'-x^2){\rm d}x\right] . \end{aligned} \tag{13}$$

Here $i=1,2$ represents the projectile and target, and $\Delta\tau_1(\mu_1')=0$,

$$\Delta\tau_2(\mu_2')=\frac{1}{2\pi^2}\left(\frac{2mT}{\hbar^2}\right)^{5/2}K_{\rm R}\left[J_1(\mu_2')-J_1(\mu_2',K_{02}^2)-K_{02}f(\mu_2',K_{02})\right]+k_{\rm R}^2\rho_2(\mu_2') .$$

From the Eqs. (11∼13), one can obtain thermal properties by inversion in principle. But such an inversion procedure is practically not feasible due to the complexity of the equations. Therefore, a more practical way is chosen to obtain the thermal properties. First, we generate all reasonable combinations T, $K_{\rm R}$ and μ_i', which ranging from $0\sim100$ MeV, $0\sim5$ fm^{-1} and $0\sim2$, respectively. Then the corresponding ρ_i,τ_i,s_i can be obtained. Second, from the extracted ρ_i,τ_i in the central region at each time step during the evolution of collision, T, $K_{\rm R}$ and μ_i' are obtained from the calculations in the first step. Third, the entropy density is calculated according to Eq. (13). One should pay attention that all the values displayed in the following pictures are the average one in the central region.

3.2 Other formula

Temperature of the system can be derived from the momentum fluctuations of particles in the center of mass frame of the fragmenting source[45]. The variance σ^2 is obtained from the Q_z distribution through

$$\sigma^2=\langle {Q_z}^2\rangle-\langle Q_z\rangle^2 , \tag{14}$$

where Q_z is the quadruple moment which is defined

by $Q_z = 2p_z^2 - p_x^2 - p_y^2$, and p_x, p_y and p_z are three components of momentum vector extracted from the phase space of BUU model. If the mean value is equal to zero, the second term vanishes. Q_z^2 is described by

$$\langle {Q_z}^2 \rangle = \int \mathrm{d}^3 p (2p_z^2 - p_x^2 - p_y^2)^2 f(p) \ . \tag{15}$$

Assuming a Maxwellian distribution for the momentum distribution, *i.e.*

$$f(p) = \frac{1}{(2\pi m T)^{3/2}} \mathrm{e}^{-\frac{{p_x}^2 + {p_y}^2 + {p_z}^2}{2mT}} \ , \tag{16}$$

we can obtain

$$\langle Q_z^2 \rangle = 4m^2 A^2 T^2 \tag{17}$$

after Gaussian integral, where m is the mass of a nucleon and A is the mass number of the fragment. For a nucleonic system, we have $A = 1$ and can calculate the evolution of temperature using this equation. Fig. 2(b) shows the temperature's evolution after 25 fm/c, it is seen that temperature reaches a maximum around 50 fm/c when the system is in the most compressible stage and then it starts to cool down when the system expands, later on the system tends thermodynamic equilibrium. For an equilibrated system,

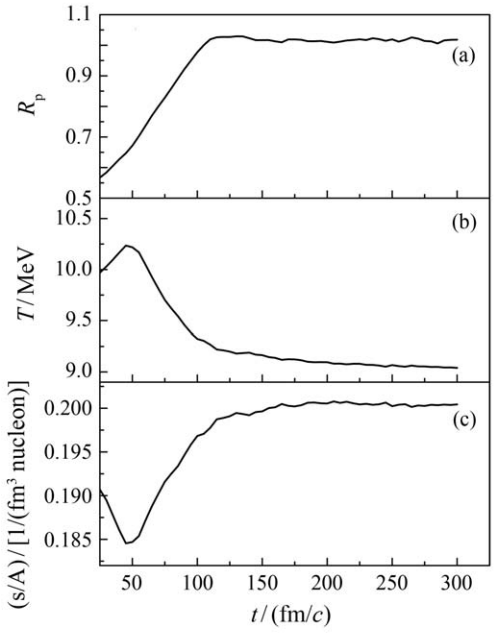

Fig. 2　R_p (a), temperature (b) and entropy density per nucleon (c) as a function of time (after 24 fm/c) for the head-on Au+Au collision within 5 fm-radius sphere at 50 MeV/u.

the kinetic energy distributions approach the Boltzmann distribution as time increases. After the expansion process, the system will approach an equilibrate state, then we can proceed to investigate the viscosity coefficient and entropy density in system.

Shear viscosity determines the strength of the energy momentum fluctuation of dissipative fluxes about the equilibrium state, which can be calculated by using Green-Kubo relation. The Green-Kubo formula for shear viscosity is defined by[53]

$$\eta = \frac{1}{T} \int \mathrm{d}^3 r \int_0^\infty \mathrm{d}t \langle \pi_{ij}(0,0) \pi_{ij}(\boldsymbol{r}, t) \rangle \ , \tag{18}$$

where T is the temperature of the system, "0" represents the starting time when the system tends to equilibrium and t is the post-equilibration time, $\langle \pi_{ij}(0,0) \pi_{ij}(\boldsymbol{r}, t) \rangle$ is the shear component of the energy momentum tensor. In order to compute an integral, we assume that nucleons are uniformly distributed in the space. Meanwhile, the isolated spherical volume with the radius of 5 fm is fixed, so the viscosity becomes

$$\eta = \frac{V}{T} \langle \pi_{ij}(0)^2 \rangle \tau_\pi \ , \tag{19}$$

where τ_π is calculated by

$$\langle \pi_{ij}(0) \pi_{ij}(t) \rangle \propto \exp(-\frac{1}{\tau_\pi}) \ . \tag{20}$$

In this work, the post-equilibration stage is defined as the nuclear matter within the given central region has reached an equilibrium which can be judged by the stopping parameter[54]. The stopping R_p is defined as

$$R_\mathrm{p} = \frac{2 \sum R_\mathrm{t}}{\pi \sum R_z} \ , \tag{21}$$

where $R_\mathrm{t} = \sqrt{p_x^2 + p_y^2}$ and $R_z = \sqrt{p_z^2}$ is the transverse and parallel momentum, respectively. Nevertheless, the anisotropy ratio can also be used to determine the equilibrium of the system. Anisotropy ratio is defined as

$$R_\mathrm{p} = \frac{2}{\pi} \frac{R_\parallel}{R_\perp} \ , \tag{22}$$

where $R_\parallel = \langle \sqrt{p_x^2 + p_y^2} \rangle$ and $R_\perp = \langle \sqrt{p_z^2} \rangle$ are calculated by the momentum of nucleons in the given volume. Fig. 2(a) shows the anisotropy ratio R_p as

a function of time for the head-on Au+Au collisions with a 5 fm-radius sphere at 50 MeV/u.

Except temperature, other thermodynamic variables can be calculated during heavy-ion collisions. Energy density inside a volume with the 5 fm-radius can be defined as

$$\varepsilon = \frac{1}{V}\sum_{r_i<r_0} E_i, \tag{23}$$

where E_i is $\sqrt{p_i^2+m_i^2}$, r_i is the position of the i-th nucleon in the center of mass and r_0 is the selected radius (here we set r_0 = 5 fm) and pressure can be defined as

$$P = \frac{1}{3V}\sum_{r_i<r_0} \frac{p_i^2}{E_i}. \tag{24}$$

After we get the energy density, pressure and temperature, entropy density can be calculated by the Gibbs formula

$$s = \frac{\varepsilon + P - \mu_{\rm n}\rho}{T}, \tag{25}$$

where $\mu_{\rm n}$ is the nucleon chemical potential and ρ is nucleon density of system within the given sphere. In principal, once we have the temperature T and $f(p)$, we can fit to a Fermi-Dirac function to extract the chemical potential. However, we can assume, for simplicity, zero nucleon chemical potential, or $\mu_{\rm n}$ can be taken around 20 MeV in the present calculation[55]. Fig. 2(c) shows entropy density per nucleon as a function of time for the head-on Au+Au collisions with a 5 fm-radius sphere at 50 MeV/u.

Different kinds of combination are used to study the ratio of shear viscosity to entropy density, *e.g.*, the momentum fluctuation method and the Gibbs formula and the Green-Kubo formula are employed in the BUU model (Sec. 4.1), and the hot Thomas Fermi formulism and the Green-Kubo formula for the IQMD model (Sec. 4.2). In the following sections we will discuss all these results one by one.

In Ref. [46, 56] the nuclear shear viscosity for normal N-N cross section, has been derived from the microscopic BUU equation and can be parameterized as a function of density ρ and temperature T:

$$\eta\left(\frac{\rho}{\rho_0},T\right) = \frac{1700}{T^2}\left(\frac{\rho}{\rho_0}\right)^2 + \frac{22}{1+T^2 10^{-3}}\left(\frac{\rho}{\rho_0}\right)^{0.7} + \frac{5.8\sqrt{T}}{1+160T^{-2}}, \tag{26}$$

where η is in MeV/fm^2c, T in MeV, and $\rho_0 = 0.168$ fm^{-3}. Fig. 3 shows η as a function of T and ρ/ρ_0. One can see that η exhibits a very distinct minimum when nuclear matter density is less than normal nuclear density. And as the density increases, the transition temperature also gets larger, *e.g.* for normal density the transition temperature locates around 10 MeV, but for 2.5 times normal density it is almost 50 MeV. This conclusion is coincident with macroscopic result.

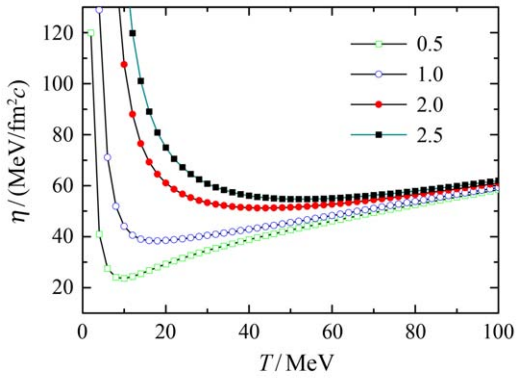

Fig. 3 (color online) Shear viscosity of nuclear matter as a function of ρ/ρ_0 and T with the Eq. (26). Different symbols represent different ρ/ρ_0, which are illustrated in the upper right corner of the figure.

4 Results and discussion

4.1 BUU results

In this section, we will show the results based on the BUU model, which are calculated by using the momentum fluctuation method and Green-Kubo formula. As already mentioned before, Fig. 2 displays the time evolution of anisotropy ratio, temperature and entropy per nucleon for Au+Au systems within a 5 fm-radius sphere at 50 MeV/u. From panel (a), it is easy to see that $R_{\rm p}$ increases from 0.5 to 1.0, this means that the system is far from equilibrium at very beginning and slowly approaches equilibrium by the interactions between the nucleons, finally around 100 fm/c the system gets equilibrated. For temperature, there is a peak around 50 fm/c, then decreases to a saturation value. As to the entropy per nucleon, it also reaches a saturation value. It is interesting to note that these three values reach their asymptotical values at the same time, which is understandable

that there should be no dramatic changes in the thermal properties when a system gets equilibrium.

Fig. 4(a) shows energy density per nucleon versus temperature for the studied system after 25 fm/c. Similarly, pressure per nucleon is shown as a function of temperature in Fig. 4(b). From the figure, we can see both energy density and pressure increase with temperature. This can be understood that in a given volume, the increasing of temperature reflects stronger thermal motion of nucleons, therefore the kinetic energy will give more contribution on energy density and pressure.

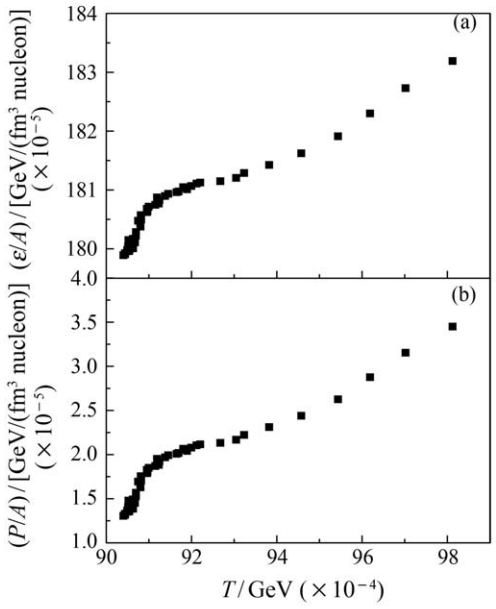

Fig. 4　Energy density per nucleon (a) and pressure per nucleon (b) as a function of temperature for the head-on Au+Au collision within 5 fm-radius sphere at 50 MeV/u.

As shown in Fig. 5(a), $\langle\pi_{ij}(0,0)\pi_{ij}(\boldsymbol{r},t)\rangle$ is plotted as a function of time for Au+Au at 50 MeV/u. The correlation function is damped exponentially with time and can be fitted by the Eq. (20) to extract the inverse slope which corresponds as the relaxation time. Fig. 5(b) shows that the relaxation time decreases as the increase of incident energy, indicating that the system can approach to equilibration faster at higher incident energy. Using the above method, we present the value of η/s as a function of incident energy after the studied system has been in equilibrium as shown in Fig. 6. The two sets of nuclear equation of state are used. The η/s value shows a rapid fall as the increasing of incident energy up to $E<70$ MeV/u and then drops slowly to a value close 0.5 when $E>70$ MeV/u. In this calculation, we did not expect to see a turning point of η/s which is usually taken as a phase transition or critical point. Since the BUU equation is a one-body theory, fragmentation which originates from the fluctuation and correlation can not be treated in the present model. In this case, the phase transition behavior cannot be predicted in the BUU model.

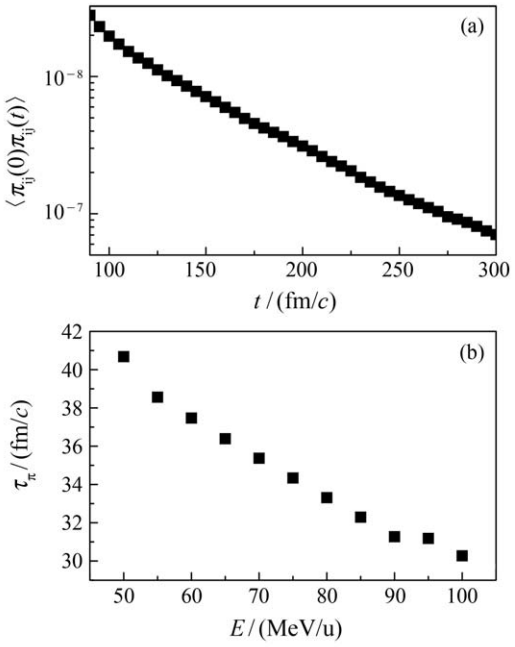

Fig. 5　(a) $\langle\pi_{ij}(0,0)\pi_{ij}(\boldsymbol{r},t)\rangle$ evolves with time for the head-on Au+Au collision in a given 5 fm-radius volume at 50 MeV/u; (b) Relaxation time as a function of incident energy for the head-on Au+Au collision in a given 5 fm-radius volume.

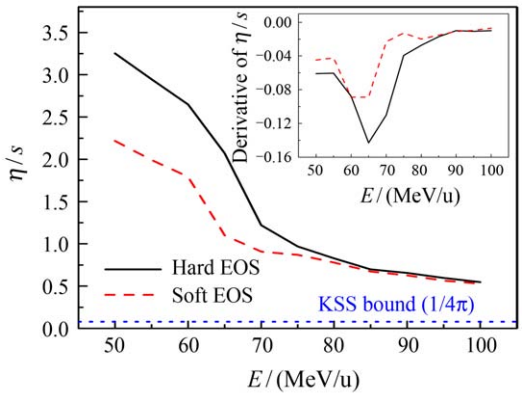

Fig. 6　(color online) η/s as a function of beam energy for the head-on Au+Au collision in a spherical volume with radius of 5 fm. The inset shows the derivative of η/s versus beam energy.

4.2 QMD results

Based on a generalized hot Thomas-Fermi formalism (GHTFF), the time evolutions of temperature and entropy density are depicted in Fig. 7. Along the time scale of the collision, one can see that both values almost evolve isochronously, reach their maxima at about 20 fm/c. After the compression stage the nuclear system begins to expand and some nucleons escape from the central region, and the central region becomes cooled down. The entropy density decreases more quickly than temperature, this is due to direct effect of the quick escape of the nucleons.

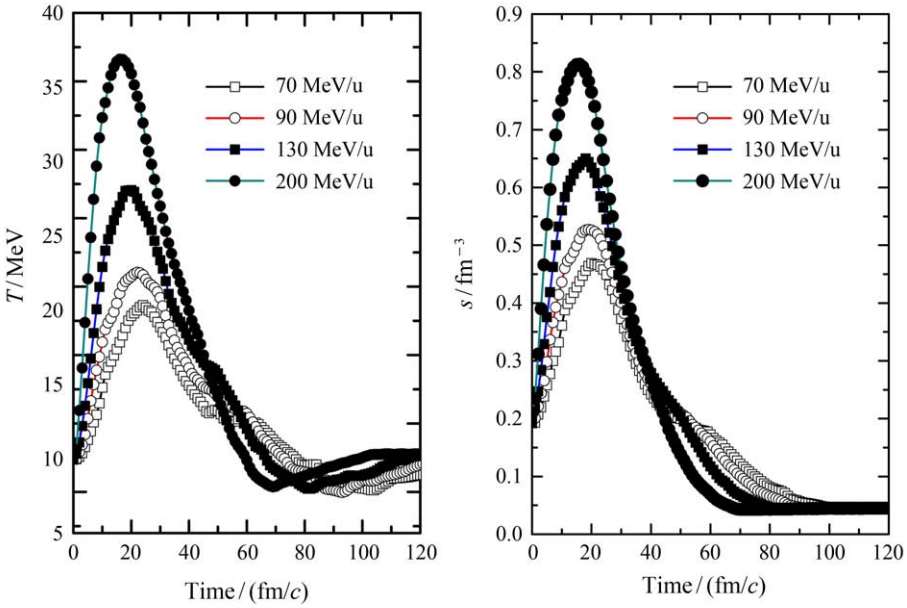

Fig. 7 Time evolution of temperature (a) and entropy density (b) in the central region. Different symbols represents different beam energy as illustrated in the inset.

Furthermore with the help of coalescence mechanism, the fragment information can be given in IQMD. The intermediate mass fragment which is here defined with charge number greater than 3 and smaller than 1/3 of the system size is very important for nuclear multi-fragmentation. These fragments are larger than typical evaporated light particles and smaller than the residues and fission products, and they can be considered as nuclear fog. So the multiplicity of intermediate mass fragments (M_{IMFs}) is related to the occurrence of liquid gas phase transition. Usually the M_{IMFs} increases first as beam energy increases when the nuclear liquid phase is still dominant, and reaches a maximum, then decreases when the nuclear gas phase becomes dominant[47]. Fig. 8 shows the M_{IMFs} which is extracted from the final stage of the collision as a function of beam energy for head-on Au+Au collisions. One can see the turning energy is around 90 MeV/u.

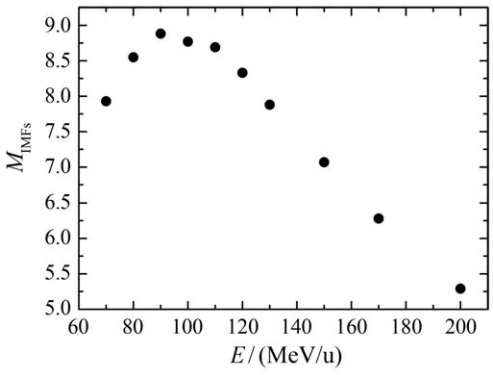

Fig. 8 M_{IMFs} as a function of beam energy for the head-on Au+Au collisions.

Time evolution of stopping is displayed in Fig. 9. From the figure, we observe that at the the initial stage the stopping is very small and its value decreases with the energy. Later there is a quick increase of the stopping due to the interplay of two body collision, mean field and Pauli blocking, and the collective motion energy turns into thermal en-

ergy and the potential energy during the compression stage. It is interesting to see there is a vibration of $R_{\rm p}$, this is caused by the transformation between the potential energy and kinetic energy. The stopping approaches a saturate value very close to 1 after oscillation, which means the nucleonic system in the central volume is very close to equilibrium in later stage of collisions. Different starting time ("0") when $R_{\rm p}$ tends to 1 has been used in the Eq. (18) for calculating viscosity.

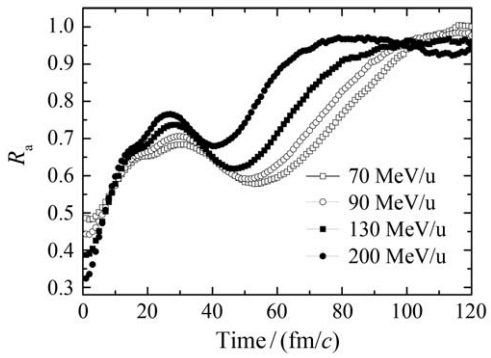

Fig. 9　Time evolution of stopping in the central sphere.
Different symbols represent different beam energy as illustrated in the inset.

As shown in Fig. 10, $\langle\pi_{ij}(0,0)\pi_{ij}(\boldsymbol{r},t)\rangle$ is plotted versus time for Au+Au collision at different incident energies. The correlation function is damped exponentially with time and can be fitted by the Eq. (20) to extract the inverse slope which corresponds to the relaxation time. Fig. 10 shows that the relaxation time decreases with the incident energy, indicating that the system approaches to equilibration faster at

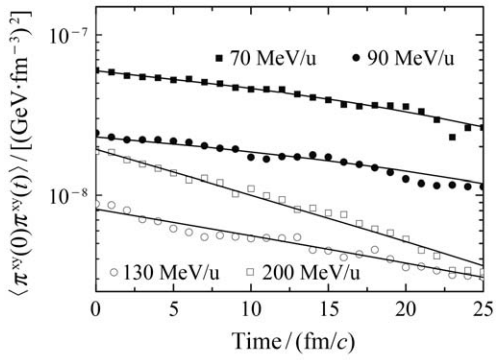

Fig. 10　$\langle\pi_{ij}(0,0)\pi_{ij}(\mathbf{r},t)\rangle$ evolves with the post-equilibration time for the head-on Au+Au collision in the central sphere. Different symbols represent different beam energies and lines are the fits with Eq. (20).

higher incident energy, which is consistent with the results from the stopping parameter.

Finally, we come by the shear viscosity and its ratio to entropy density. Fig. 11(a) shows shear viscosity η as a function of incident energy. It is very interesting to see that the shear viscosity alone also exhibits a minimum near 120 MeV/u. Since the temperatures in post-equilibration stage are almost the same for the collisions at different energies, the values of shear viscosity are mostly influenced by the tensor correlation, which reflects the fluctuation of dissipative fluxes. Fig. 11(b) displays η/s as a function incident energy for the head-on Au+Au collisions from 70 to 200 MeV/u. The η/s decreases quickly with the incident energy up to a platform of the minimum value at around 120 MeV/u and

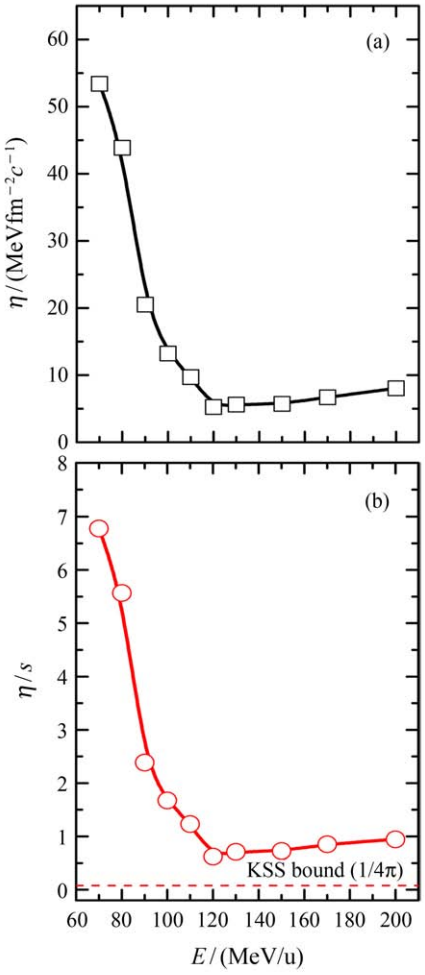

Fig. 11　Shear viscosity η (a) and the ratio of shear viscosity to entropy density (b) as a function of incident energy for the head-on Au+Au collisions.

afterwards the curve weakly rise up slowly. The minimum value is around 0.6, *i.e.* about 7 times KSS bound ($1/4\pi$). As we expected, all η/s values from the present QMD model are lager than the KSS bound. On the other hand, we noticed that the location of energy with the maximum $N_{\rm IMFs}$ and η/s is not exactly the same, it might be due to our Green-Kubo calculation focuses on a given central nuclear region, and the IMFs represent the whole colliding system.

5 Summary

Thermodynamical and transport properties of a fireball formed in head-on Au+Au collisions are investigated in both IQMD and BUU model. The ratio of shear viscosity to entropy density is explored by different methods, mainly including the hot Thomas-Fermi formulism, the momentum fluctuation method, Green-Kubo formula, Danielewicz's parameterized function. A minimum is found for the ratio of shear viscosity to entropy density in IQMD, and while an asymptotic saturation value was observed in BUU. We argue that a minimum or saturation η/s corresponds to a liquid gas phase transition of nuclear system in the intermediate energy heavy-ion collisions.

References:

[1] DAS GUPTA S, MEKJIAN A Z, TSANG M B. Adv Nucl Phys, 2001, **26**: 89.

[2] BONASERA A, BRUNO M, DORSO C O, *et al.* Riv Nuovo Cimento, 2000, **23**: 1.

[3] BORDERIE B, RIVET M F. Progr Part Nucl Phys, 2008, **61**: 551.

[4] POCHODZALLA J, MOHLENKAMP T, RUBEHN T, *et al* (ALADIN Collaboration). Phys Rev Lett, 1995, **75**: 1040.

[5] MA Y G, SIWEK A, PETER J, *et al.* Phys Lett B, 1997, **390**: 41.

[6] NATOWITZ J B, HAGEL K, MA Y G, *et al.* Phys Rev Lett, 2002, **89**: 212701.

[7] GROSS D H E. Rep Prog Phys, 1990, **53**: 605.

[8] BONDORF J P, BOTVINA A S, *et al.* Phys Rep, 1995, **257**: 133.

[9] MA Y G, SHEN W Q. Nucl Sci Tech, 2004, **15**: 4; ZHANG G Q, CAO X G, FU Y, *et al.* Nucl Sci Tech, 2012, **23**: 61.

[10] GILKES M L, ALBERGO S, BIESER F, *et al.* Phys Rev Lett, 1994, **73**: 1590.

[11] ELLIOTT J B, GILKES M L, HAUGER J A, *et al.* Phys Rev C, 1994, **49**: 3185; Phys Rev Lett, 2002, **88**: 042701.

[12] MA Y G, Phys Rev Lett, 1999, **83**: 3617; Eur Phys J A, 2006, **30**: 227; Ma Y G, WADA R, HAGEL K, *et al.* Phys Rev C, 2004, **69**: 031604(R); Phys Rev C, 2005, **71**: 054606.

[13] FISHER M E, Rep Prog Phys, 1969, **30**: 615; Physics, 1967, **3**: 255.

[14] GULMINELLI F, D'AGOSTINO M. Eur Phys J, A, 2006, **30**: 253.

[15] LOPEZ O, RIVET M F. Eur Phys J A, 2006, **30**: 263.

[16] CSERNAI L P, KAPUSTA J I, MCLERRAN L D. Phys Rev Lett, 2006, **97**: 152303.

[17] KOVTUN P K, SON D T, STARINETS A O. Phys Rev Lett, 2005, **94**: 111601.

[18] POLICASTRO G, SON D T, STARINETS A O. Phys Rev Lett, 2001, **87**: 081601.

[19] DEMIR N, BASS S A. Phys Rev Lett, 2009, **102**: 172302.

[20] LACEY R, AJITAN N N, ALEXANDER J M, *et al.* Phys Rev Lett, 2007, **98**: 092301.

[21] CHEN Jiunnwei, NAKANO E. Phys Lett B, 2007, **647**: 371.

[22] KAPUSTA J I, SPRINGER T. Phys Rev D, 2008, **78**: 066017.

[23] SONG H, BASS S A, HEINZ U, *et al.* Phys Rev Lett, 2011, **106**: 192301.

[24] SHI L, DANIELEWICZ P. Phys Rev C, 2003, **68**: 064604.

[25] PAL S. Phys Lett B, 2010, **684**: 211; Phys Rev C, 2010, **81**: 051601(R).

[26] AUERBACH N, SHLOMO S. Phys Rev Lett, 2009, **103**: 172501.

[27] LI S X , FANG D Q, MA Y G, *et al.* Phys Rev C, 2011, **84**: 024607; Nucl Sci Tech, 2011, **22**: 235.

[28] ZHOU C L, MA Y G, FANG D Q, *et al.* Europhys Lett, 2012, **98**: 66003.

[29] ZHOU C L, MA Y G, FANG D Q, *et al.* Phys Rev C, 2013, **88**: 024604.

[30] XU Jun, Phys Rev C, 2011, **84**: 064603.

[31] XU J, CHEN L W, KO C M, *et al.* Phys Lett B, 2013, **727**: 244.

[32] AICHELIN J. Phys Rep, 1991, **202**: 233.

[33] HARTNACK C, LI Zhuxia, NEISE L, *et al.* Nucl Phys A, 1989, **495**: 303c.

[34] HARTNACK C, RAJEEV K. PURI J, *et al.* Eur Phys J A, 1998, **1**: 151.

[35] MA Y G, WEI Y B, SHEN W Q, *et al.* Phys Rev C, 2006, **73**: 014604.

[36] WANG J, MA Y G, *et al.* Nucl Sci Tech, 2013, **24**, 030501.

[37] TAO C, MA Y G, ZHANG G Q, *et al.* Nucl Sci Tech, 2013, **24**: 030502.

[38] BERTSCH G F. Michigan State University Cyclotron Laboratory preprint, MSUCL-544 (1985).
[39] WONG C Y, TANG H H K. Phys Rev Lett, 1978, **40**: 1070.
[40] BAUER W, BERTSCH G F, CASSING W, *et al*. Phys Rev C, 1986, **34**: 2127.
[41] BERTSCH G F, DAS GUPTA S. Phys Rep, 1988, **160**: 189.
[42] KHOA D T, OHTSUKA N, FAESSLER A, *et al*. Nucl Phys A, 1992, **542**: 671.
[43] KHOA D T, OHTSUKA N, FAESSLER A, *et al*. Nucl Phys A, 1992, **548**: 102.
[44] PURI P K, OHTSUKA N, LEHMANN E, *et al*. 1992 GSI Scientific Report 93-1, GSI, Darmstadt, Germany, p. 126.
[45] WUENSCHEL S, BONASERA A, MAYA L W, *et al*. Nucl Phys A, 2010, **843**: 1; ZHENG Hua, BONASERA A, Phys Lett B, 2011, **696**: 178.
[46] DANIELEWICZ P. Phys Lett B, 1984, **146**: 168.
[47] MA Y G, SHEN W Q. Phys Rev C, 1995, **51**: 710.
[48] PEASLEE G F, TSANG M B, SCHWAR Z C, *et al*. Phys Rev C, 1994, **49**: R2271.
[49] OGILVIE C A, ADOLFF J C, BEGEMANN-BLAICH M. *et al*. Phys Rev Lett, 1991, **67**: 1214.
[50] TSANG M B, HSI W C, LYNCH W G, *et al*. Phys Rev Lett, 1993, **71**: 1502.
[51] BARRANCO M, TREINER J. Nucl Phys A, 1981, **351**: 269.
[52] RASHDAN M, FAESSLER A, ISMAIL M, *et al*. Nucl Phys A, 1987, **468**: 168.
[53] KUBO R. Rep Prog Phys, 1966, **29**: 255.
[54] ZHANG G Q, MA Y G, CAO X G, *et al*. Phys Rev C, 2011, **84**: 034612.
[55] KONOPKA J, GRAF H, STÖCKER H, *et al*. Phys Rev C, 1994, **50**: 2085.
[56] DANIELEWICZ P, BARKER B, SHI L J. AIP Conf Proc, 2009, **1128**: 104.

中能重离子碰撞中参与者区域的粘滞系数与熵密度之比

马余刚[1)]，周铖龙，方德清

(中国科学院上海应用物理研究所，上海　201800)

摘要： 在同位旋依赖的量子分子动力学 (IQMD) 和 Boltzmann-Uehling-Uhlenbeck(BUU) 的框架下研究了重离子碰撞过程中核物质的剪切粘滞系数与熵密度的比值。用不同的方法提取了剪切粘滞系数 (η)、熵密度 (s) 和其他相关的物理量。随着碰撞能量的增加，粘滞系数和熵密度的比值在 BUU 模型中逐渐趋于一个饱和值而在 IQMD 模型中出现了一个极小值，认为这个局域的最小值或饱和值对应于中能重离子碰撞中发生的核物质液气相变现象。

关键词： 剪切粘滞系数；熵密度；重离子碰撞；输运模型

收稿日期： 2013-09-25；　**修改日期：** 2013-10-18

基金项目： 国家自然科学基金资助项目(11035009, 11220101005)，国家重点基础研究发展计划 (973计划) 项目(2013CB834405))

1)　E-mail：ygma@sinap.ac.cn。